



## A fast pointwise strategy for anisotropic wave-mode separation in TI media

Item Type	Conference Paper
Authors	Liu, Qiancheng;Peter, Daniel;Lu, Yongming
Citation	Liu Q, Peter D, Lu Y (2017) A fast pointwise strategy for anisotropic wave-mode separation in TI media. SEG Technical Program Expanded Abstracts 2017. Available: <a href="http://dx.doi.org/10.1190/segam2017-17795796.1">http://dx.doi.org/10.1190/segam2017-17795796.1</a> .
Eprint version	Publisher's Version/PDF
DOI	<a href="http://dx.doi.org/10.1190/segam2017-17795796.1">10.1190/segam2017-17795796.1</a>
Publisher	Society of Exploration Geophysicists
Journal	SEG Technical Program Expanded Abstracts 2017
Rights	Archived with thanks to SEG Technical Program Expanded Abstracts 2017
Download date	2025-03-22 06:09:02
Link to Item	<a href="http://hdl.handle.net/10754/626220">http://hdl.handle.net/10754/626220</a>

## A fast pointwise strategy for anisotropic wave-mode separation in TI media

Qiancheng Liu\* and Daniel Peter, King Abdullah University of Science and Technology (KAUST), Physical Science and Engineering Division (PSE)  
Yongming Lu, Institute of Geology and Geophysics, Chinese Academy of Sciences

### Summary

The multi-component wavefield contains both compressional and shear waves. Separating wave-modes has many applications in seismic workflows. Conventionally, anisotropic wave-mode separation is implemented by either directly filtering in the wavenumber domain or nonstationary filtering in the space domain, which are computationally expensive. These methods could be categorized into the pseudo-derivative family and only work well within Finite Difference (FD) methods. In this paper, we establish a relationship between group-velocity direction and polarity direction and propose a method, which could go beyond modeling by FD. In particular, we are interested in performing wave-mode separation in a Spectral Element Method (SEM), which is widely used for seismic wave propagation on various scales. The separation is implemented pointwise, independent of its neighbor points, suitable for running in parallel. Moreover, no correction for amplitude and phase changes caused by the derivative operator is required. We have verified our scheme using numerical examples.

### Introduction

For most seismic applications, Earth can be considered as an elastic solid with anisotropy which arises, e.g., from ordered heterogeneity at much smaller scales than the seismic wavelength. Thus, a good approximation to describe realistic wave propagation in the Earth is given by solving the anisotropic elastic wave equation. Anisotropic wave-mode separation dates back to Dellinger and Etgen (1990) in the wavenumber domain. They establish a relationship between phase-velocity direction and polarity direction according to the Christoffel equation. Yan and Sava (2009) suggest in VTI media to construct the corresponding spatial filter instead of wavenumber filter, and then convolve the Cartesian wavefield components to conduct wave-mode separation.

To alleviate the computational cost, Cheng and Fomel (2014) use low-rank approximations to the projection relation between phase-velocity direction and polarization direction. Also, it is well known that after the wave-mode separation by a derivative operator, the amplitude of the wavefield is scaled by a factor depending on the ratio of frequency and local phase velocity. Furthermore, the phase is rotated by 90 degrees. Both effects need to be corrected.

In this paper, we will tie a numerical relationship between group-velocity direction and polarity direction and then perform wave-mode separation according to the polarity direction. We will also show that although the directions of wave propagation are in four quadrants, only the relationship in one quadrant is enough to describe the relationship. We will easily promote our scheme from VTI to TI with a simple additional tilt rotation.

### Anisotropic elastic wave equation and Poynting vector (group velocity vector)

The anisotropic elastic wave equation reads

$$\rho \frac{\partial v_i}{\partial t} = \frac{\partial \tau_{ij}}{\partial x_j}, \quad (1)$$

$$\frac{\partial \tau_{ij}}{\partial t} = \frac{1}{2} c_{ijkl} \left( \frac{\partial v_k}{\partial x_l} + \frac{\partial v_l}{\partial x_k} \right).$$

where  $\rho$  denotes density,  $\mathbf{v}$  the particle velocity,  $\boldsymbol{\tau}$  the stress tensor,  $\mathbf{x}$  the Cartesian coordinate components and  $c_{ijkl}$  the fourth-order elastic stiffness tensor. The Poynting vector  $\mathbf{p}$  which denotes the direction of group velocity (energy propagation) could be expressed as

$$\mathbf{p} = -\boldsymbol{\tau}\mathbf{v}. \quad (2)$$

It is easy to obtain  $\boldsymbol{\tau}$  and  $\mathbf{v}$  during the wavefield computation by equation (1).

### Relationship between phase-velocity vector and group-velocity vector

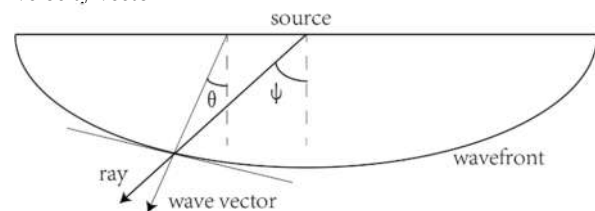


Figure 1: Illustration of the difference between phase-velocity vector (wave vector) and group-velocity vector (ray).

In 2D case, according to Berryman (1979), the relationship between phase velocity and group velocity (in figure 1) could be written as

$$\bar{V}_G = \frac{\partial(kV)}{\partial k_x} \bar{i} + \frac{\partial(kV)}{\partial k_z} \bar{j}. \quad (3)$$

in which

### Fast pointwise TI wave-mode separation

$$\begin{aligned} V_{G_x} &= \frac{\partial(kV)}{\partial k_x} = V(\theta) \cos \theta - \frac{\partial V(\theta)}{\partial \theta} \sin \theta, \\ V_{G_z} &= \frac{\partial(kV)}{\partial k_z} = V(\theta) \sin \theta + \frac{\partial V(\theta)}{\partial \theta} \cos \theta. \end{aligned} \quad (4)$$

where phase velocity  $V(\theta)$  is the function of phase angle  $\theta$ .  $V_{G_x}$  and  $V_{G_z}$  determine the direction of group velocity, which is also determined by equation (2). For simplicity, in 2D elastic case, we rewrite equation (4) as  $\psi_p = F(\theta_p)$  and  $\psi_{SV} = F(\theta_{SV})$ .

#### Relationship between phase-velocity vector and anisotropic polarization vector in VTI media

The anisotropic elastic wave equation can be written as

$$\rho \frac{\partial^2 u_i}{\partial t^2} - c_{ijkl} \frac{\partial^2 u_k}{\partial x_j \partial x_l} = 0. \quad (5)$$

where  $\mathbf{u}$  denotes particle displacement. In the harmonic plane wave approximation, we can write the solution of equation (5) as

$$\mathbf{u} = \mathbf{U} e^{i\omega(\mathbf{n}\mathbf{x}/V - t)}. \quad (6)$$

in which  $\mathbf{U}$  is the polarization vector,  $\omega$  the angular frequency,  $V$  the phase velocity,  $\mathbf{n}$  the unit vector orthogonal to the wave front. Substituting equation (6) into equation (5) yields the Christoffel equation, in 2D VTI media written as

$$\begin{bmatrix} c_{11} \cos^2 \theta + c_{55} \sin^2 \theta - \rho V^2 & (c_{13} + c_{55}) \cos \theta \sin \theta \\ (c_{13} + c_{55}) \cos \theta \sin \theta & c_{55} \cos^2 \theta + c_{33} \sin^2 \theta - \rho V^2 \end{bmatrix} \begin{bmatrix} U_1 \\ U_3 \end{bmatrix} = 0 \quad (7)$$

where we express the unit vector  $\mathbf{n}$  in terms of the phase angle  $\theta$ , that is,  $n_x = \cos \theta, n_z = \sin \theta$ . We write Equation (7) for short as

$$[\mathbf{G} - \rho V^2 \mathbf{I}] \mathbf{U} = 0. \quad (8)$$

the parameter  $V$  corresponding to the eigenvalues of the matrix  $\mathbf{G}$  represents the phase velocity of different wave modes and is a function of phase angle  $\theta$ . In 2D VTI case, the qP- and qSV-modes are uncoupled from the SH-mode and are polarized in the vertical plane. If we represent the stiffness coefficients using Thomson parameters (Thomsen, 1986; Tsvankin, 2005), the two solutions of Equation (8) can be written as

$$\begin{aligned} V_p(\theta) &= V_{p0} \sqrt{1 + \varepsilon \cos^2 \theta + \frac{a}{2} \left( \sqrt{1 + \frac{4 \cos^2 \theta}{a} (2\delta \sin^2 \theta - \varepsilon \sin 2\theta) + \frac{4\varepsilon^2 \cos^4 \theta}{a^2}} - 1 \right)}, \\ V_{sv}(\theta) &= V_{sv0} \sqrt{1 + \varepsilon \cos^2 \theta + \frac{a}{2} \left( -\sqrt{1 + \frac{4 \cos^2 \theta}{a} (2\delta \sin^2 \theta - \varepsilon \sin 2\theta) + \frac{4\varepsilon^2 \cos^4 \theta}{a^2}} - 1 \right)}. \end{aligned} \quad (9)$$

where we have

$$\begin{aligned} V_{p0} &= \sqrt{\frac{c_{33}}{\rho}}, \quad V_{sv0} = \sqrt{\frac{c_{55}}{\rho}}, \quad \varepsilon = \frac{c_{11} - c_{33}}{2c_{33}}, \\ \delta &= \frac{(c_{13} + c_{55})^2 - (c_{33} - c_{55})^2}{2c_{33}(c_{33} - c_{55})}, \quad a = 1 - \frac{V_{sv0}^2}{V_{p0}^2}. \end{aligned} \quad (10)$$

Substituting equation (9) back to equation (7) yields the polarization vector of qP- and qSV-waves:  $\mathbf{U}_p$  and  $\mathbf{U}_{SV}$ , respectively. Similar to the group-velocity angle  $\psi$  and phase-velocity angle  $\theta$ , we express the polarization angle denoted by  $\mathbf{U}_p$  and  $\mathbf{U}_{SV}$  as  $\tilde{\theta}_p$  and  $\tilde{\theta}_{SV}$ . For simplicity, in 2D elastic case, we express the relationship between phase velocity angle and polarization angle as  $\tilde{\theta}_p = f(\theta_p)$  and  $\tilde{\theta}_{SV} = f(\theta_{SV})$ .

#### Connection between polarization angle and group-velocity angle via phase-velocity angle

We already obtain the group velocity angle  $\psi$  in equation (2). Taking a P-mode for example, the question is how to get  $\tilde{\theta}_p$  from  $\psi_p$ . Our strategy is to precompute their relationship as a numerical table for each parameter combination of  $\varepsilon, \eta, a$ . We then get quick access to this numerical table during wavefield propagation. The specific implementation of this table making procedure is as follows:

1. Given a group of discrete phase-angle values, for example ranging from 0-degree to 90-degree with an even interval of 1-degree, we input the given angle  $\theta$  into Christoffel equation and obtain  $V_p(\theta)$  and  $\tilde{\theta}_p = f(\theta_p)$ .
2. Substituting  $V_p(\theta)$  into equation (4) yields  $\psi_p = F(\theta_p)$ , which shares the same variable  $\theta_p$  with  $\tilde{\theta}_p = f(\theta_p)$ . We then establish a numerical relationship bridging  $\psi_p$  to  $\tilde{\theta}_p$  by interpolation via  $\theta_p$ . The numerical table is stored in memory in advance for computational efficiency.

Similarly, we can get  $\tilde{\theta}_{sv}$  from  $\psi_{sv}$ . The reason why we only consider the partial table ranging from 0 to 90 degree rather than the full table from 0 to 360 degree is that in VTI media the relationship between  $\psi$  and  $\tilde{\theta}$  is symmetrical in four quadrants, expect for some sign differences. The sign differences could be determined by the sign characteristics of the Poynting vector in four quadrants. If necessary, we could ignore the numerical table at 0 and 90 degrees because even in an anisotropic media the waves are not polarized along the symmetry axis  $x$  and  $z$ .

#### Pointwise wave-mode separation

## Fast pointwise TI wave-mode separation

Since a P wave is longitudinal and S wave is transverse, once obtaining  $\tilde{\theta}$  from  $\psi$ , we perform wave-mode separation as following:

$$\begin{aligned} U_p &= v_x \cos \tilde{\theta} + v_z \sin \tilde{\theta}, \\ U_{sv} &= -v_x \sin \tilde{\theta} + v_z \cos \tilde{\theta}. \end{aligned} \quad (11)$$

where  $v_x$  and  $v_z$  are particle velocities in equation (1),  $U_p$  and  $U_{sv}$  are separated potential wavefields. Note that although the polarization vectors of qP and qSV are orthogonal, the corresponding group velocity vectors are not. Hence it is necessary to tell apart qP from qSV. Here we use a simple strategy by first carrying out a global wave-mode separation using polarization angle  $\tilde{\theta}_p$ . Then, we evaluate the ratio  $\alpha$  of the global S-wave energy and the original wavefield energy on each point as following:

$$\alpha = |U_{sv}| / \sqrt{v_x^2 + v_z^2}. \quad (12)$$

If a successful qP wave separation has been done, hardly any qSV energy will be left. Note that some stabilization is required in the above division. We judge the wave-mode according to  $\alpha$ . If  $\alpha$  is less than some threshold, for example 0.01, we mark the wave on the corresponding point as qP wave. Next, we continue the wave-mode separation using  $\tilde{\theta}_{sv}$  for the points left. Since the separation is done with a projection along the polarization direction rather than by a pseudo-derivative operator, the amplitude scale won't change and the phase characteristic of the original wavefield remains intact. Moreover, because it is a pointless separation independent of its neighbor points, this separation is much easier to run in parallel compared with conventional pseudo-derivative methods.

### Wave-mode separation in TI media

The wave-mode separation scheme presented here could also be extended to transverse isotropy with a tilted symmetry axis (TTI) media, without the requirement to solve a TTI Christoffel equation, which is more difficult than the VTI one. Physically, the TTI media is a rotation of a VTI media. Therefore, assuming the tilt is  $\beta$ , we first rotate the group-velocity angle  $\psi$  by  $\beta$  back to the symmetrical axis, in which we just solve a VTI Christoffel equation to get the numerical relationship between  $\psi$  and  $\tilde{\theta}$  in the rotated coordinate system, and then rotate  $\tilde{\theta}$  by  $-\beta$  to return back to the TTI media.

### Analysis on computational storage and efficiency

We could directly extend our method to heterogeneous media by precomputing and storing numerical tables for qP and qSV at every grid point. The storage cost of this

method is  $N$  by  $2 \times nb$  in a linear relationship, where  $N$  is the model size and  $nb$  is the size of the numerical table. However, this might lead to implementation problems. To further reduce the memory cost, we precompute the distribution of the model parameters  $\varepsilon, \eta, a$  in advance. Note that the tilt parameter is not required in the establishment of the numerical table. Consequently, we could sample the space spanned by  $\varepsilon, \eta, a$  within the effective domain. This way the memory storage will be significantly reduced, especially for simple media. Another strategy would be to analyze the parameter sensitivity for a given model. Then, for insensitive parameters a larger sampling interval could be chosen.

The numerical table with respect to  $\varepsilon, \eta, a$  is stored in memory, such that there is no need to re-calculate it again. The additional computational costs are caused by the calculation of Poynting vector and the wave-mode separation by polarization angle  $\tilde{\theta}$ . Only some additional multiplications and additions are required. The wave-mode is pointwise. The computational cost and the model size are also related linearly.

### Examples

In this part we consider two groups of models to verify our method. Both of them have the same  $V_p=3000\text{m/s}$ ,  $V_s=2000\text{m/s}$ ,  $\text{Density}=2400\text{kg/m}^3$ . In the first group, we have  $\text{Epsi}=0.3$ ,  $\text{Delta}=0.1$ ,  $\text{Tilt}=45$  degree; in the second group, we have  $\text{Epsi}=0.1$ ,  $\text{Delta}=0.2$ ,  $\text{Tilt}=45$  degree. The Poynting vectors, X and Z components, separated qP and qSV waves corresponding to different parameters, are shown in figures 2 and 3, respectively. Note that in our method, qP and qSV waves are separated well with no change of amplitude and phase caused.

### Conclusions

We propose a pointwise anisotropic wave-mode separation method based on the relationship between polarization vector and group velocity vector (Poynting vector). The anisotropic separation scheme presented here overcomes the limitation of mode-separation being only feasible in a Finite Difference Method. Our scheme allows to be performed on unstructured mesh based modelling methods, thus becomes amenable for e.g. a Spectral Element Method (SEM). Although the process of formula derivation is tedious, the final relationship is brief and simple. Compared with conventional pseudo-derivative methods, our method keeps both amplitude scale and phase of the original wavefield intact, and is independent on neighboring points. The size of the numerical table and the additional computational costs are linearly related to model size.

### Fast pointwise TI wave-mode separation

Furthermore, our method is applicable to general TI media such as VTI, HTI, TTI media.

#### Acknowledgement

The research reported in this publication was supported by funding from King Abdullah University of Science and Technology (KAUST). Numerical computations used resources of the IT Division and Extreme Computing Research Center (ECRC) at KAUST.

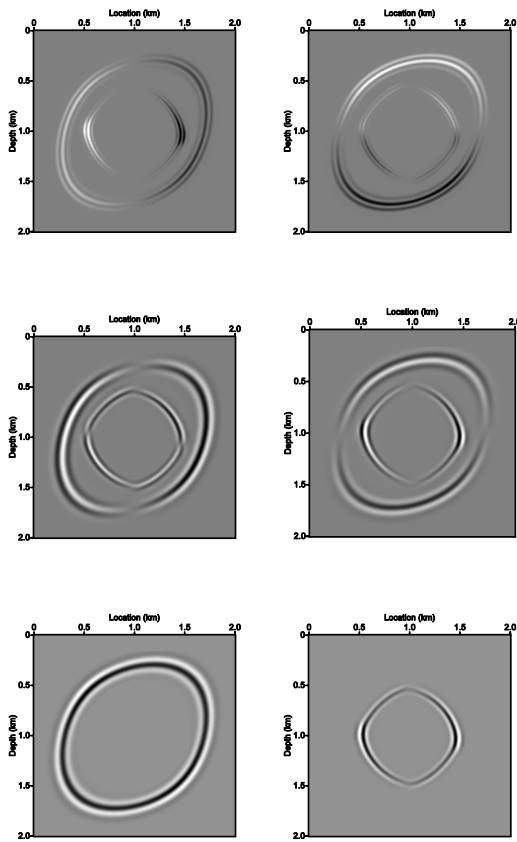


Figure 2: Top row: Poynting vector. Middle row: X and Z components  
Bottom row: Separated qP and qSV components (Epsi=0.3, Delta=0.1, Tilt=45 degree).

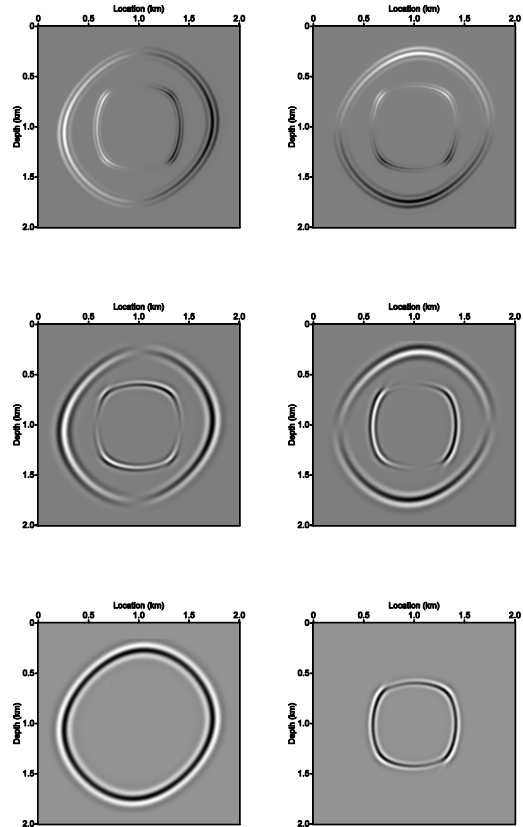


Figure 3: Top row: Poynting vector. Middle row: X and Z components  
Bottom row: Separated qP and qSV components (Epsi=0.1, Delta=0.3, Tilt=45 degree).

#### EDITED REFERENCES

Note: This reference list is a copyedited version of the reference list submitted by the author. Reference lists for the 2017 SEG Technical Program Expanded Abstracts have been copyedited so that references provided with the online metadata for each paper will achieve a high degree of linking to cited sources that appear on the Web.

#### REFERENCES

- Berryman, J. G., 1979, Long-wave elastic anisotropy in transversely isotropic media. *Geophysics*, **44**, 896–917, <http://dx.doi.org/10.1190/1.1440984>.
- Cheng, J., and S. Fomel, 2014, Fast algorithms for elastic-wave mode separation and vector decomposition using low-rank approximation for anisotropic media: *Geophysics*, **79**, C97–C110, <http://dx.doi.org/10.1190/geo2014-0032.1>.
- Dellinger, J., and J. Etgen, 1990, Wave-field separation in two-dimensional anisotropic media. *Geophysics*, **55**, 914–919, <http://dx.doi.org/10.1190/1.1442906>.
- Thomson, L., 1986, Weak elastic anisotropy: *Geophysics*, **51**, 1954–1966, <http://dx.doi.org/10.1190/1.1442051>.
- Tsvankin, I., 2005, *Seismic signatures and analysis of reflection data in anisotropic media* (2nd ed.): Elsevier.
- Yan, J., and P. Sava, 2009, Elastic wave-mode separation for VTI media: *Geophysics*, **74**, WB19–WB32, <http://dx.doi.org/10.1190/1.3184014>.